# Supramolecular Coordination Chemistry

CHEMICAL REVIEWS

Review

pubs.acs.org/CR

## Recent Developments in the Preparation and Chemistry of Metallacycles and Metallacages via Coordination

Timothy R. Cook*,† and Peter J. Stang*,‡

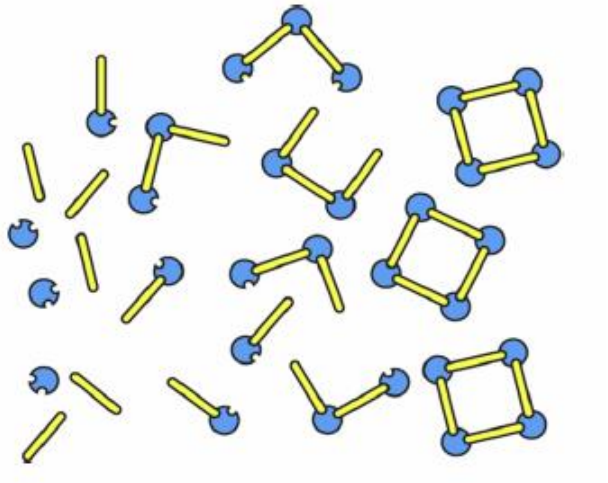

Chem. Rev. **2015**, *115*, 7001.

# Advantages of Using Transition-Metal Complexes for the Construction of Supramolecular Assemblies

- Transition metal-ligand interactions can be quite **strong** (typically between 40 and 120 k*J*/mol).
- Transition metal-ligand interactions are **highly directional**.
- Ligands can undergo **fast exchange reactions** (error correction is possible).
- The unique properties of transition metals can add some **function** to the supramolecular assembly (color, redox activity, etc…).

# A $Pd(en)^{2+}$-Based Molecular Square

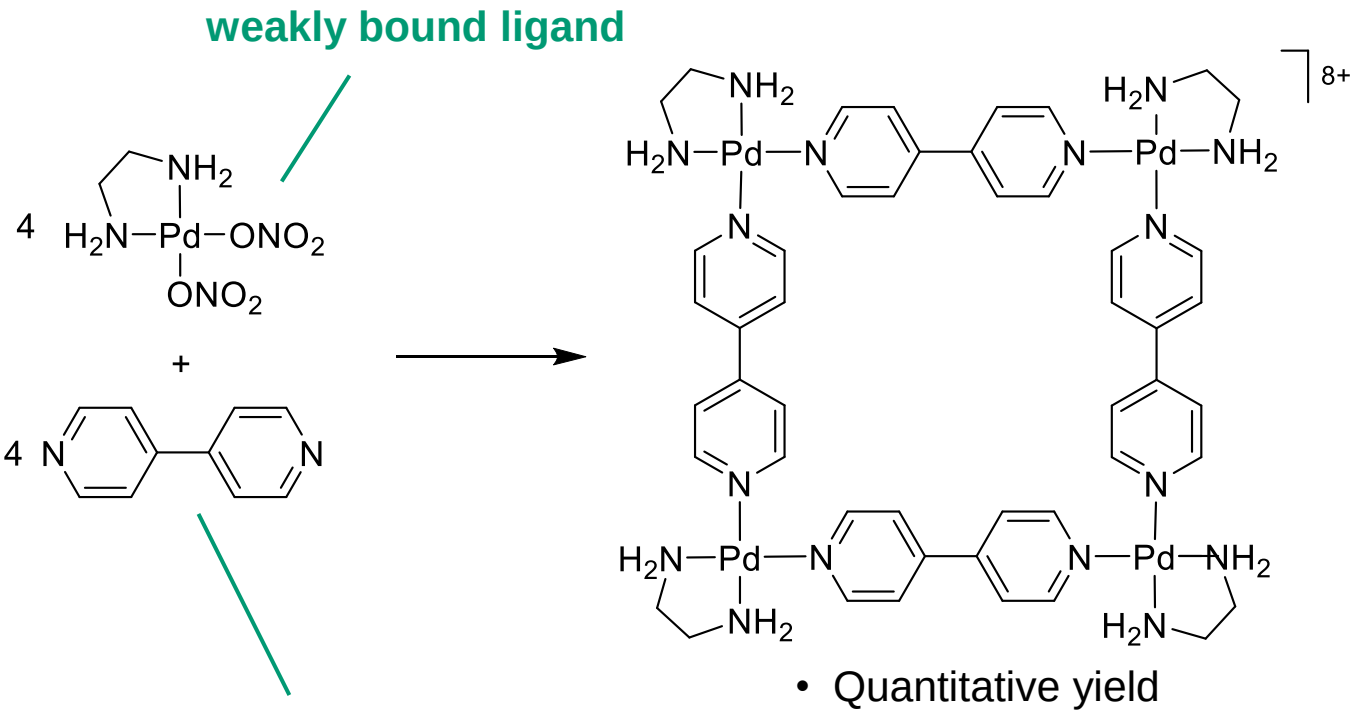


- Quantitative yield
- Water soluble
- Only one set of NMR signals
- Structure confirmed by X-ray
- With $Pt^{2+}$ the reaction takes weeks!

M. Fujita et al. *J. Am. Chem. Soc.* **1990**, *112*, 5645.

# Generalization

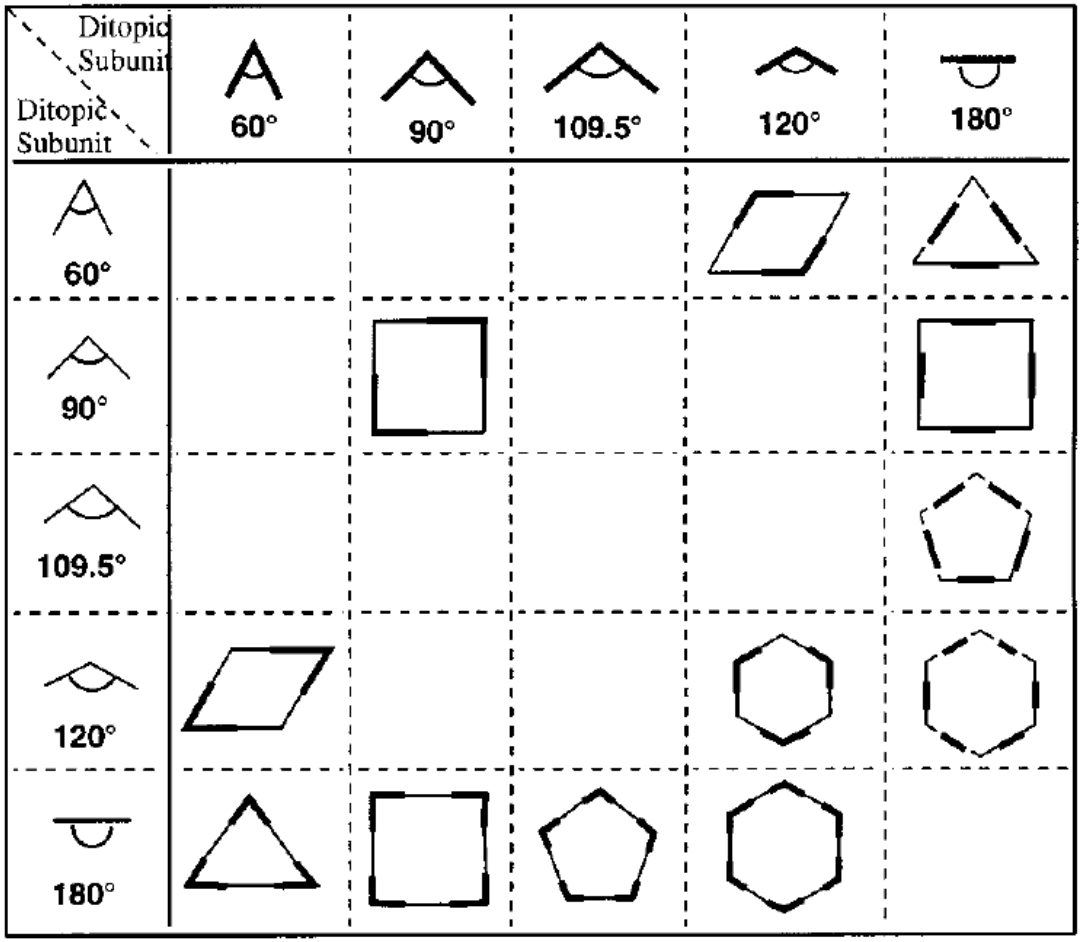


Macrocycles created via the systematic combination of ditopic building blocks with predetermined angles.

# Thermodynamic Considerations

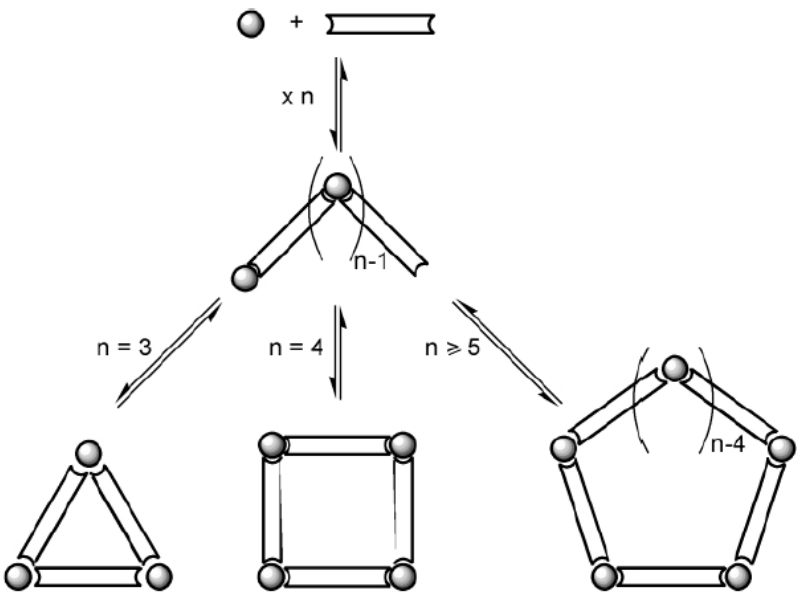


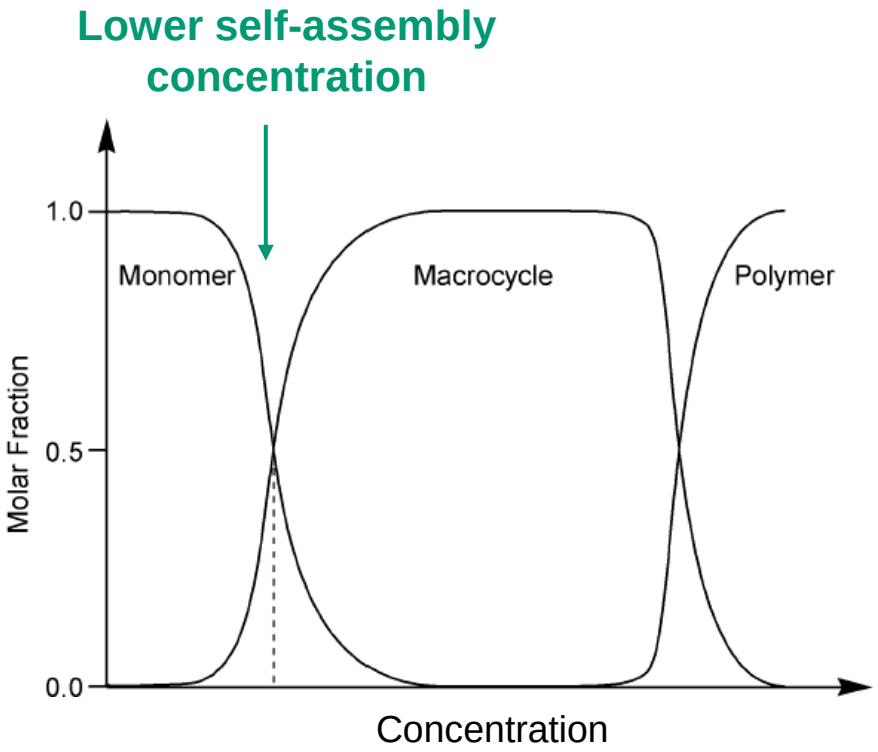


The desired macrocyclic products exist as major species only within a limited range of concentration under given temperature and solvent conditions. In order to accomplish self-assembly already at low concentration, the coordinative bonds should exhibit considerable thermodynamic stability.

# Trimer-Tetramer Equilibrium

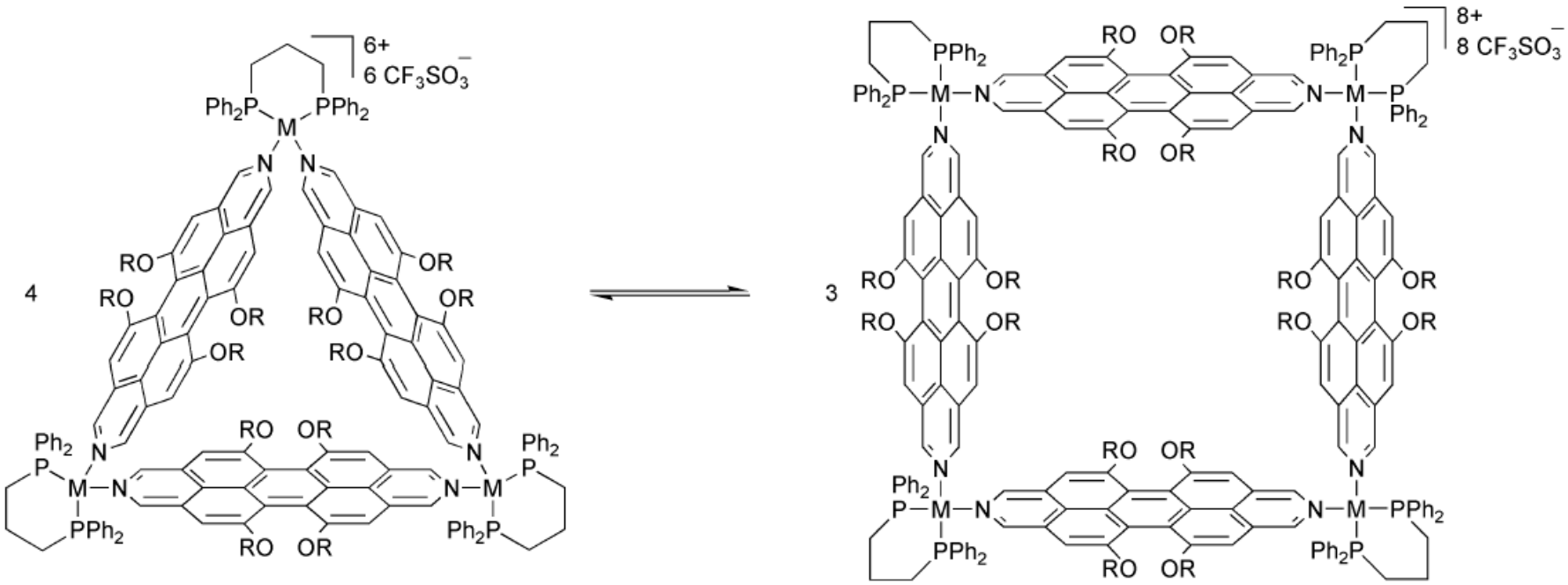


From the viewpoint of thermodynamics, **enthalpy favors the formation of squares** which have less conformational strain (90° corner) than triangles (60° corner), while **entropy favors the formation of triangles** which are assembled from fewer components than squares. As a consequence, both the triangular and square species may co-exist in solution.

# Ligands as Corners

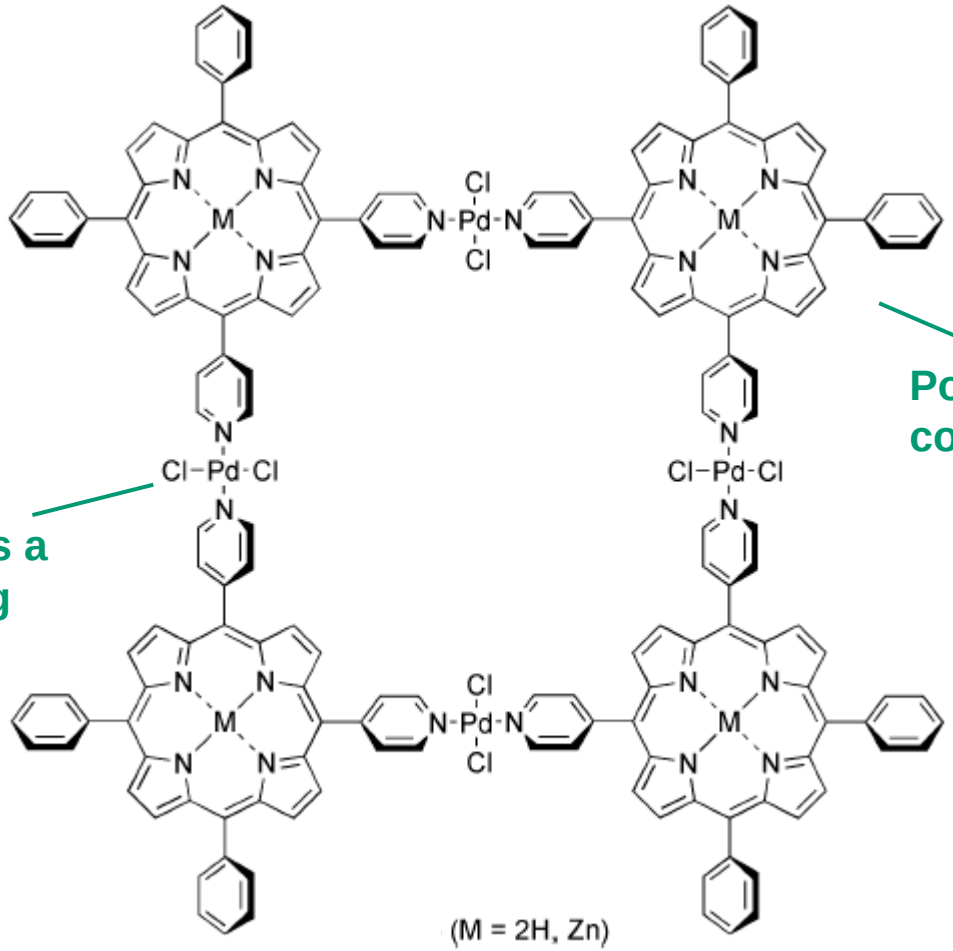


Porphyrin as a 90 ° corner

Metal complex as a linear connecting unit

# Molecular Squares Based on Octahedral Complexes

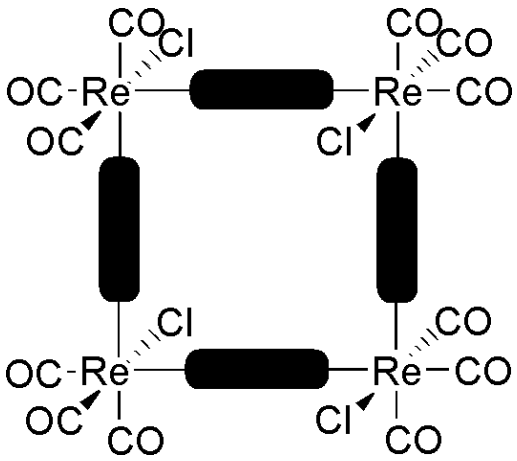


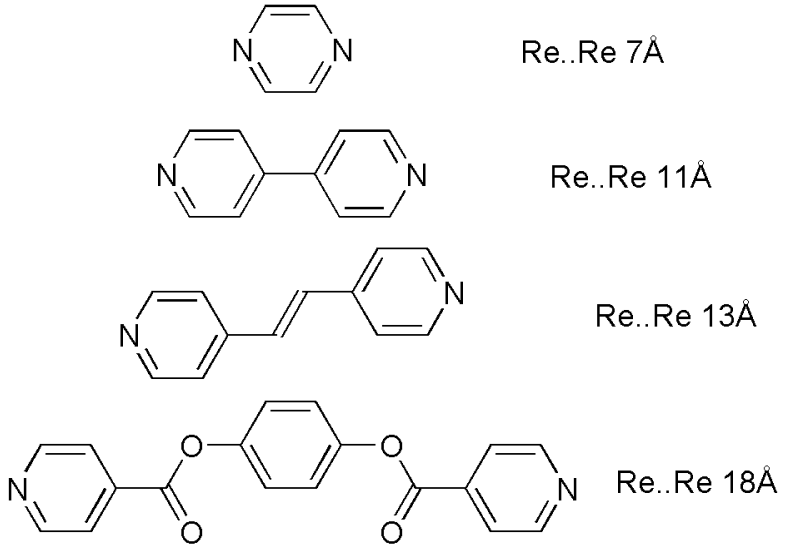


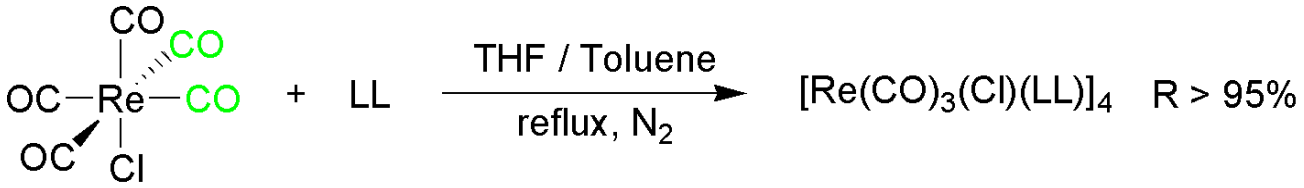


J. T. Hupp et al., *Inorg. Chem.* **1996**, *35*, 4096.

# 3-D Coordination Cages

| Tritopic Subunit \ Ditopic Subunit | 80-90° | 109° | 180° |
|---|---|---|---|
| 60° | | 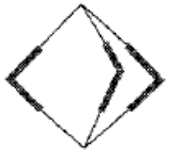 trigonal bipyramide |  tetrahedron |
|  90° |  trigonal bipyramide | | 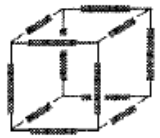 cube |
|  109.5° |  "double square" |  adamantanoid | 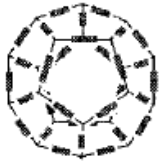 dodecahedron |
|  120° |  truncated tetrahedron |  cuboctahedron | |

3-D cages are created via the systematic combination of ditopic with tritopic building blocks.

# A $Pd(en)^{2+}$-Based $M_6L_4$ Cage

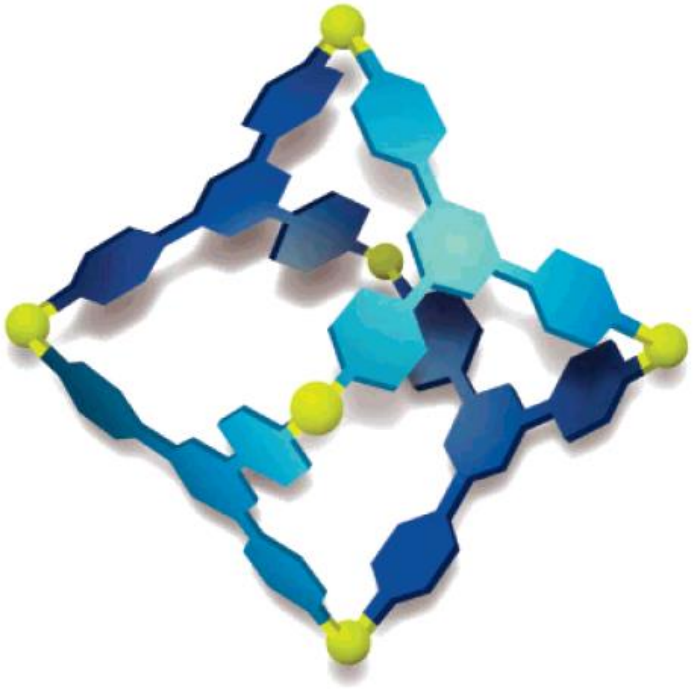

- Mixing the ligand and $[(en)Pd(NO_3)_2]$ in water in a 3:2 ratio.
- The cage is amphiphilic; the outside is hydrophilic due to the presence of six cationic Pd(II) centers making the cage highly water-soluble, whereas the inside is hydrophobic.
- The molecular recognition within the cage can be easily monitored by NMR (guest signals are highly upfield shifted).


M. Fujita et al., *Nature* **1995**, *378*, 469.

# Sequence-Selective Recognition of Peptides by a $Pd(en)^{2+}$-Based $M_6L_4$ Cage

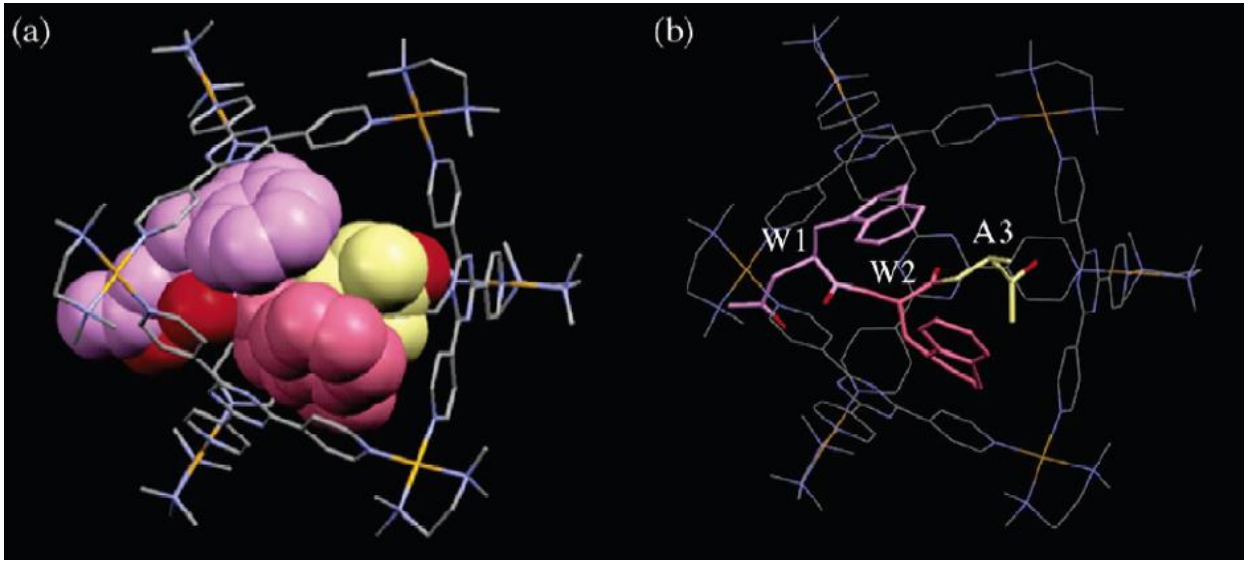


**Cage + Trp-Trp-Ala (X-Ray)**

The coordination cage recognizes oligopeptides in a highly sequence-selective fashion. In particular, the Trp-Trp-Ala sequence is strongly bound by the cavity ($K_a$ = $10^6$ $M^{-1}$). Tripeptides possessing the same residues but in different sequences (i.e., Trp-Ala-Trp and Ala-Trp-Trp) show much poorer affinity. NMR and X-ray analyses reveal that the sequence-selective recognition is ascribed to cooperative multiple interactions between the residues and the hydrophobic cavity.

M. Fujita et al., *J. Am. Chem. Soc.* **2005**, *127*, 4546.

# A Ru-Based Molecular Cube

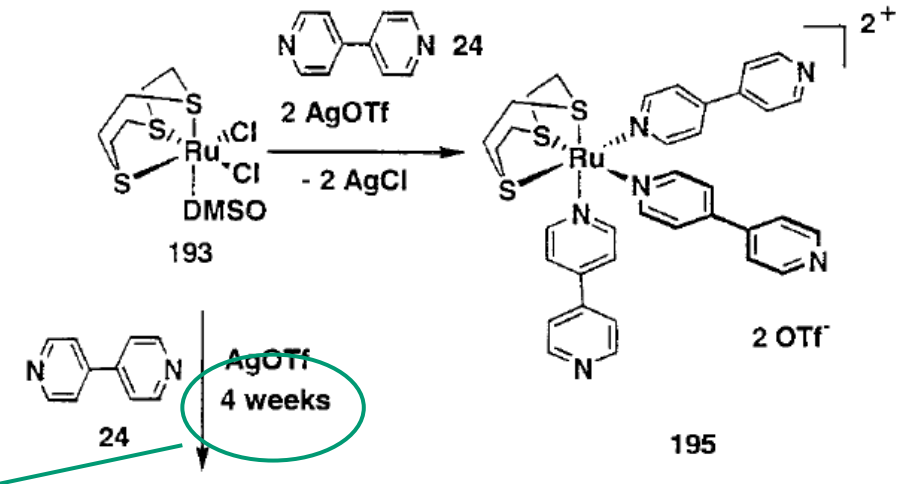


Exchange reactions at the 4d metal Ru are slow

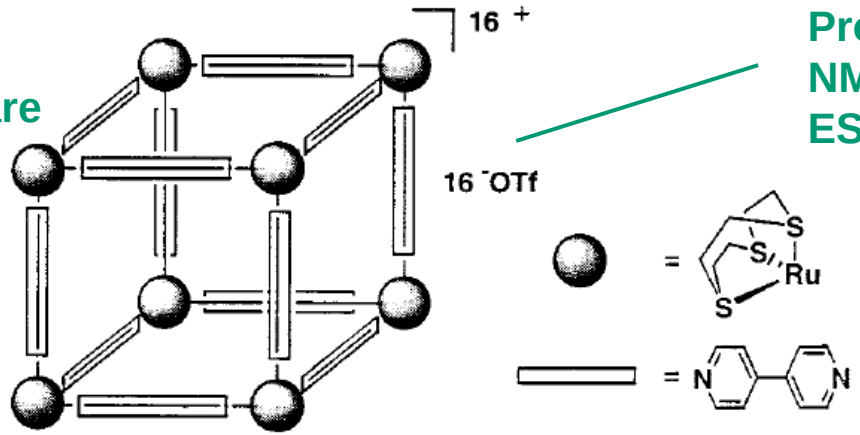


Product characterized by NMR, elemental analysis and ES-MS.

J. A. Thomas et al., *Chem. Commun.* **1998**, 1681.

# Coordination Barrels

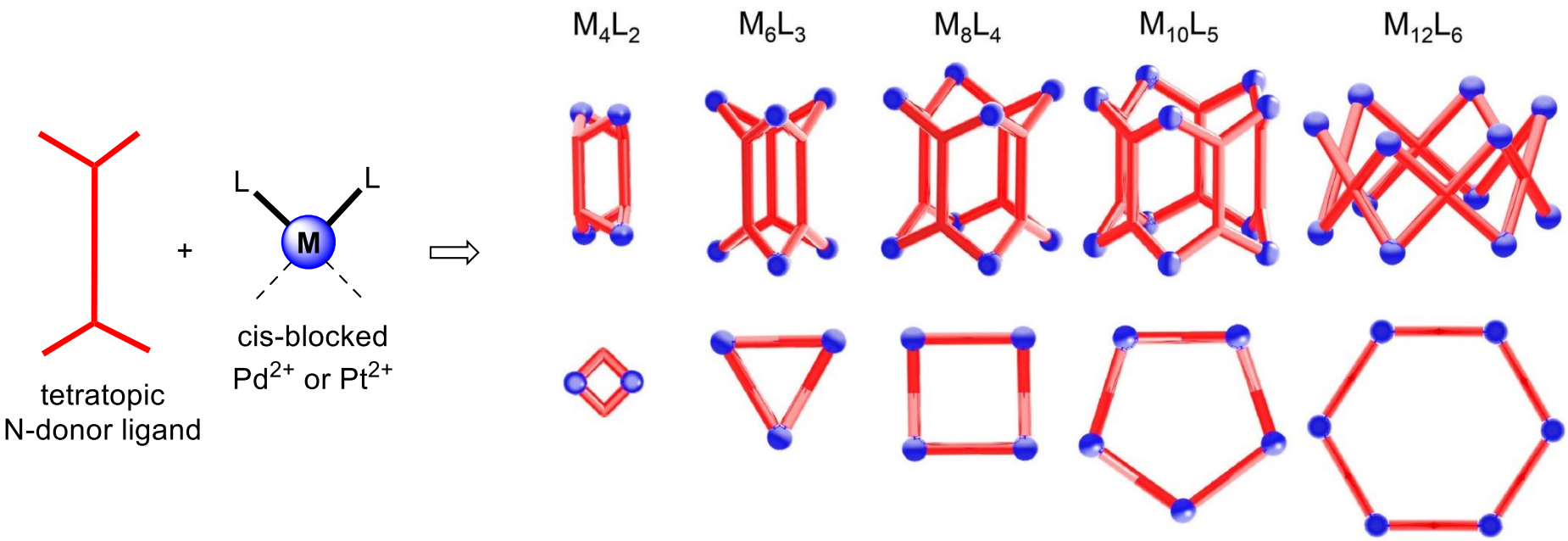


K. Severin et al., *J. Am. Chem. Soc.* **2017**, *139*, 8371.

# Coordination Barrels – Potential Ligands

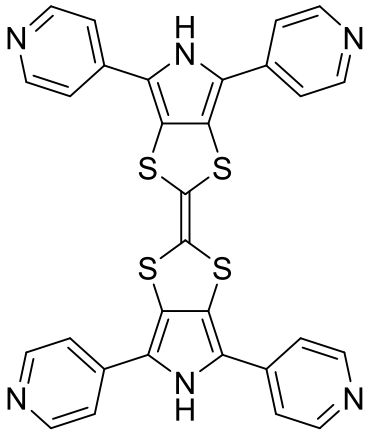


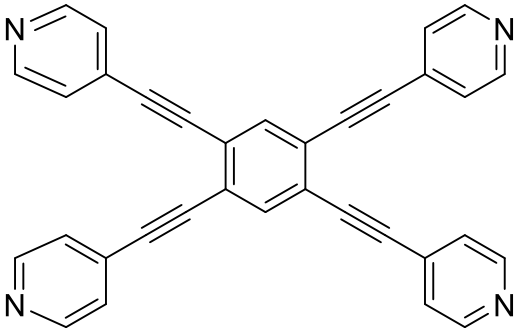


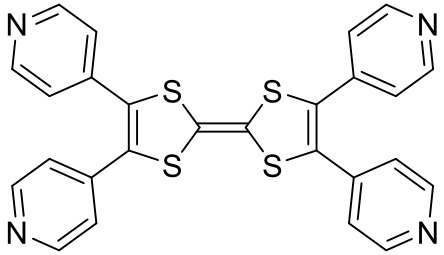


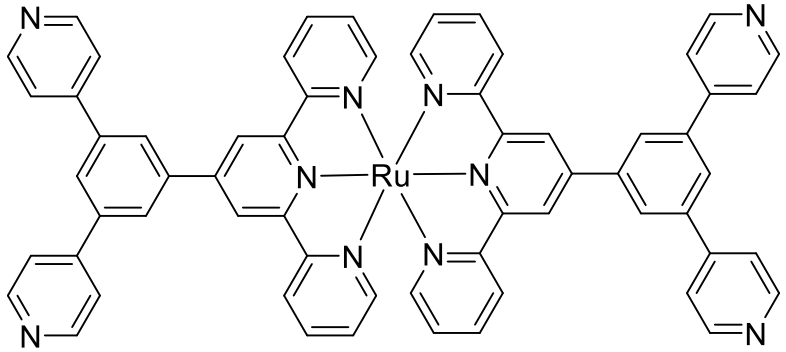


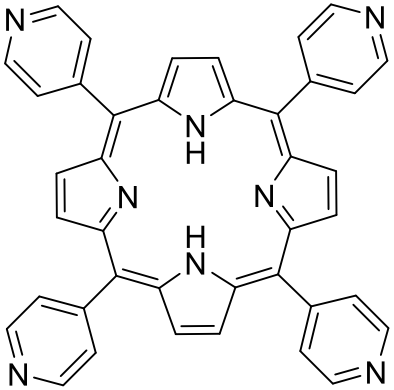

# A $Pd(en)^{2+}$-Based Coordination Nanotube

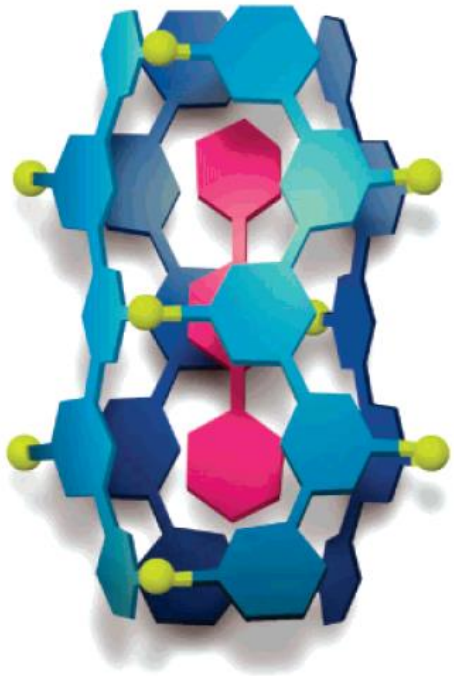

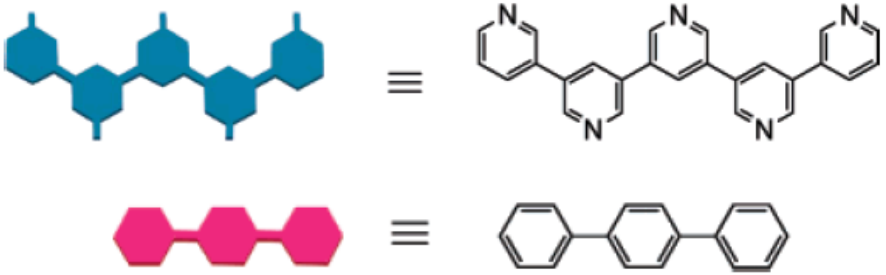


The nanotube consists of four ligands and 10 molecules of $(en)Pd^{2+}$. The guest *p*-terphenyl is bound via $\pi-\pi$ and CH-$\pi$ interactions.

M. Fujita et al., *J. Am. Chem. Soc.* **1999**, *121*, 7457 .

# Cages Based on ‘Naked’ Metal Ions

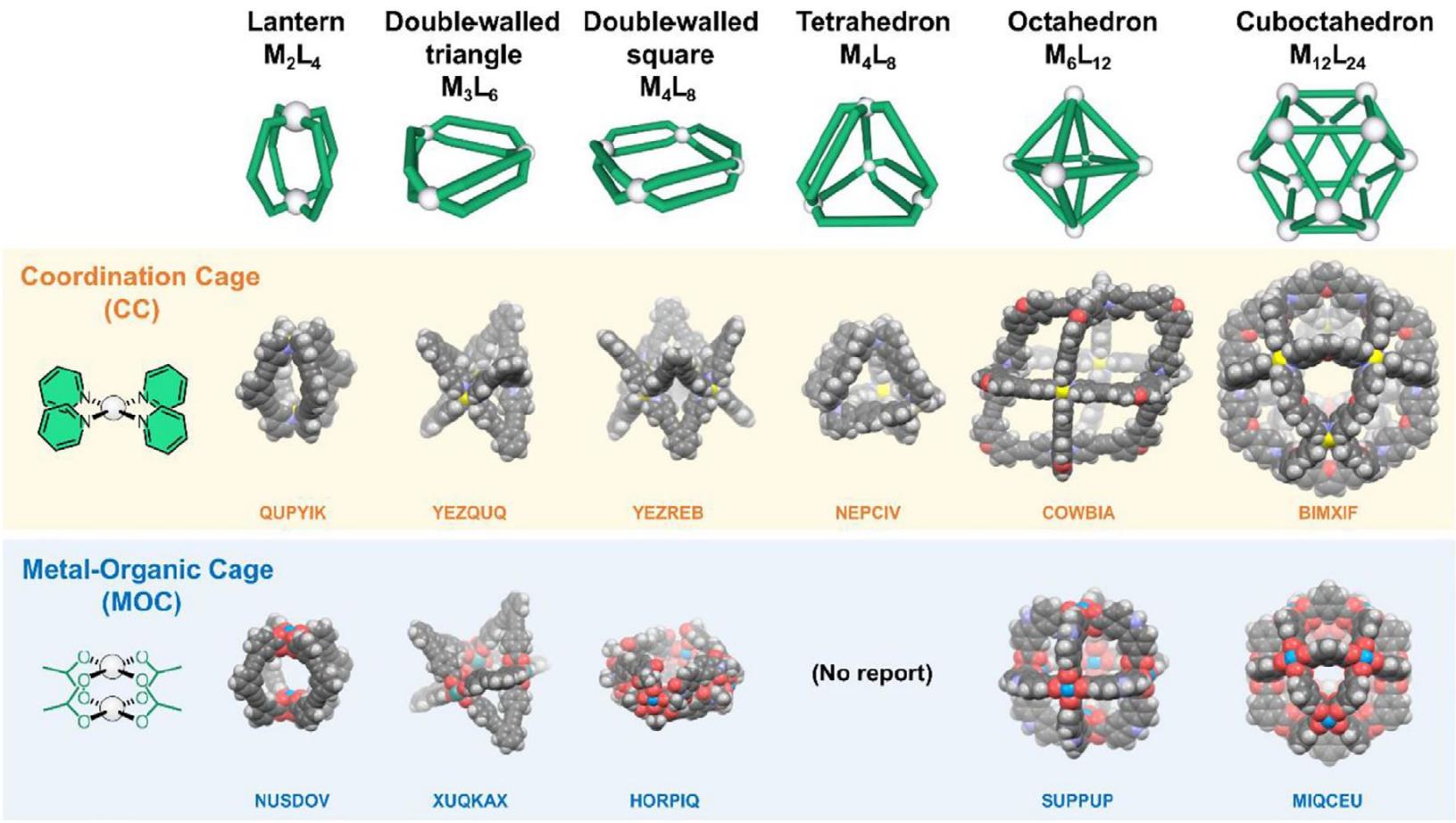


S. Furukawa et al., *Coord. Chem. Rev.* **2022**, *467*, 214612.

# The Geometry of the Ligand

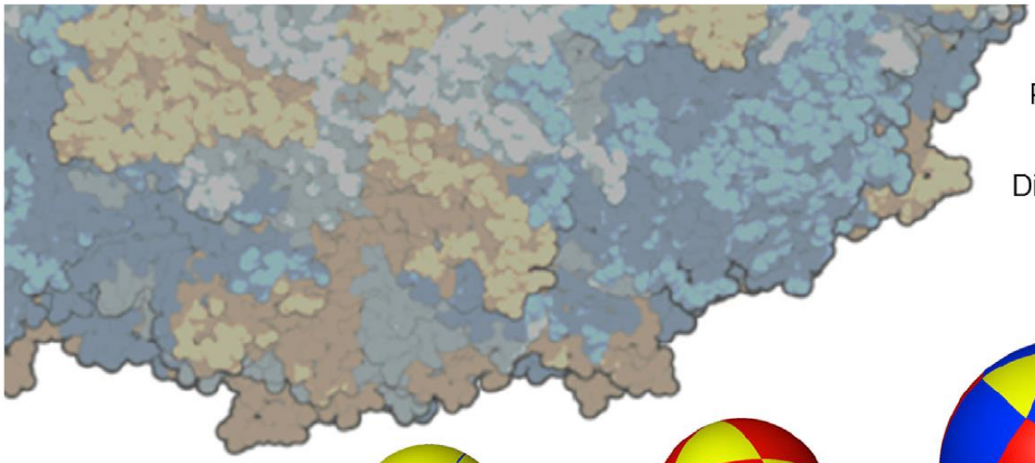

Poliovirus ($I_h$)
$L_{60}$
Diameter: 30 nm

Scale / nm
10
9
8
7
6
5
4
3
2
1
0

| | | | | |
|---|---|---|---|---|
| **Polyhedron** | Octahedron ($O_h$) | Cuboctahedron ($O_h$) | Rhombicuboctahedron ($O_h$) | Icosidodecahedron ($I_h$) |
| **Stoichiometry** | $M_6L_{12}$ | $M_{12}L_{24}$ | $M_{24}L_{48}$ | $M_{30}L_{60}$ |
| **Ideal Angle** | 90° | 120° | 135° | 150° |
| **Ligand** | 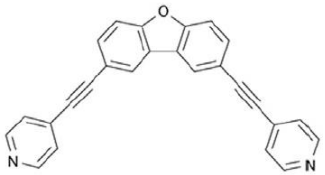 | 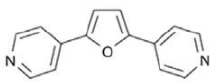 | 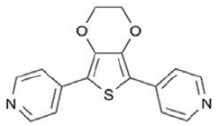 | 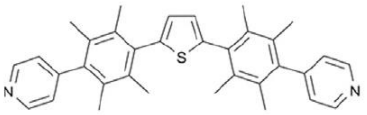 |

Review: B. S. Pilgrim and J. R. Nitschke, *Chem.* **2022**, *1*, 19.

# Iminopyridine Ligands

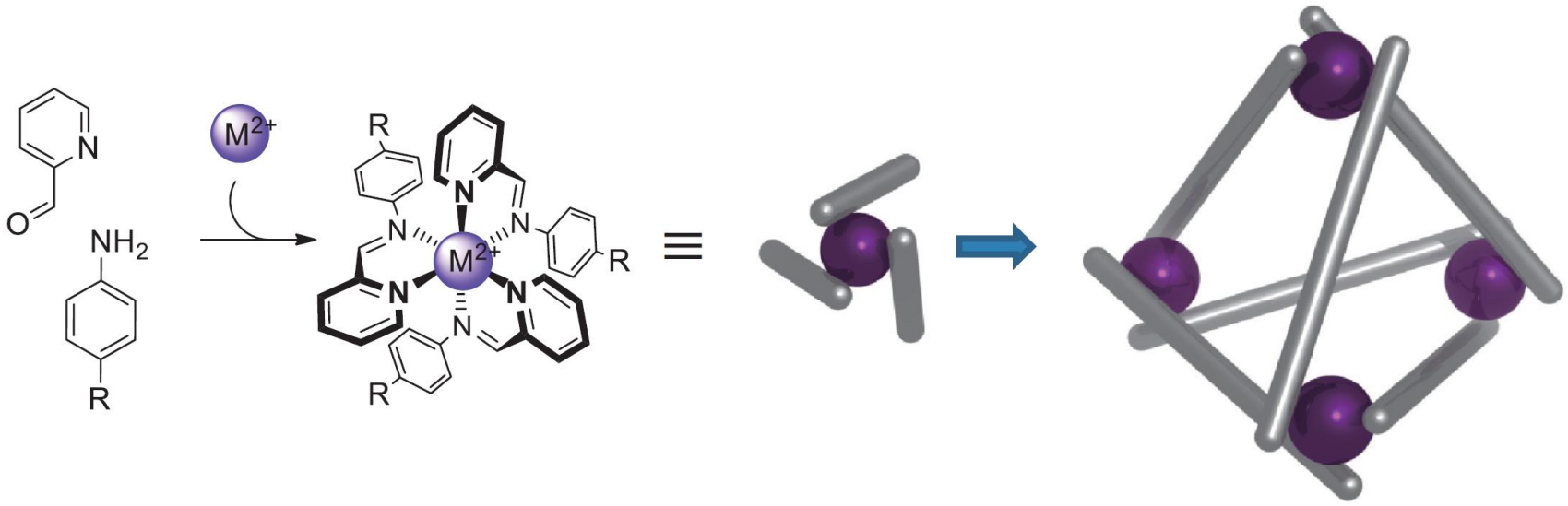

# Iminopyridine Ligands

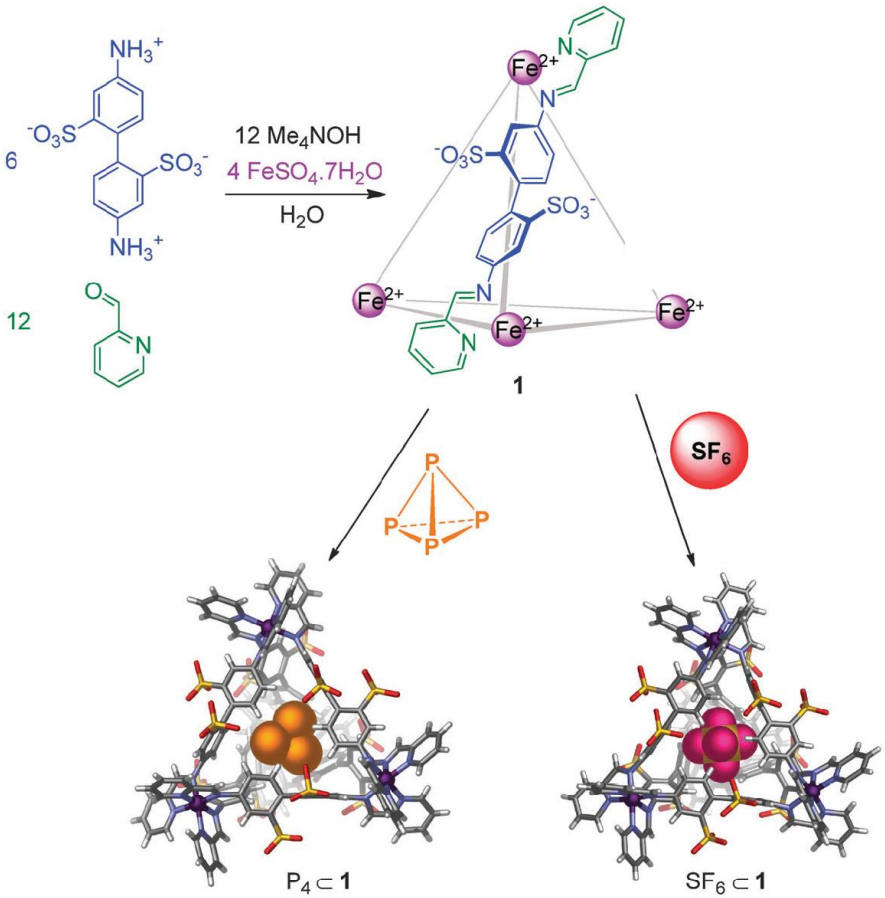


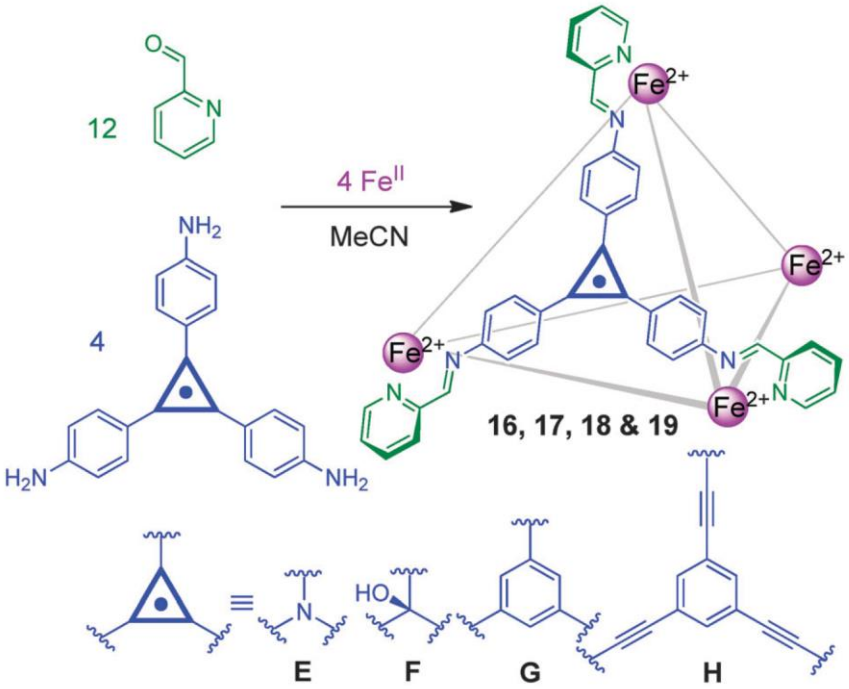


J. R. Nitschke et al., *Chem. Commun.* **2013**, *49*, 2476.

# Catecholate Ligands

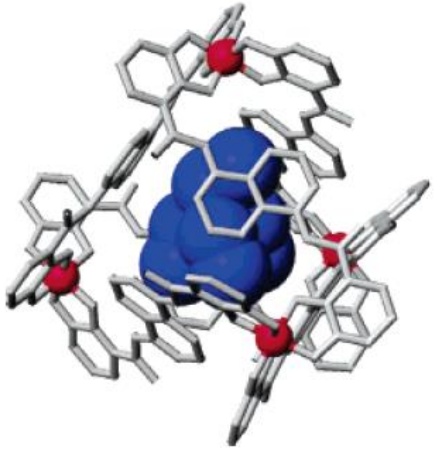

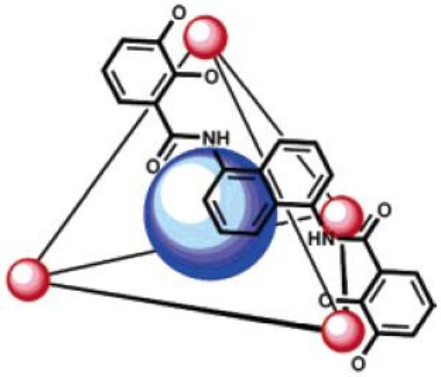


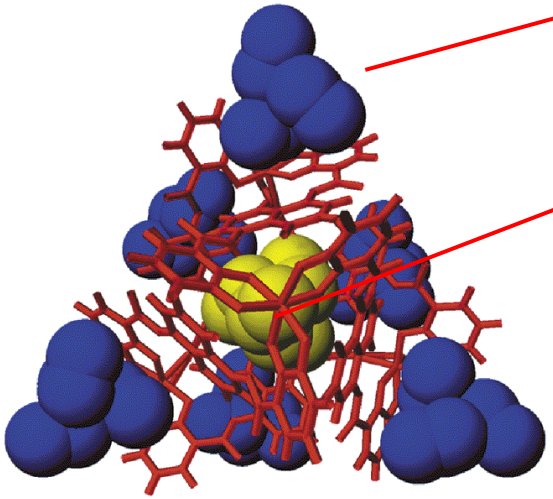

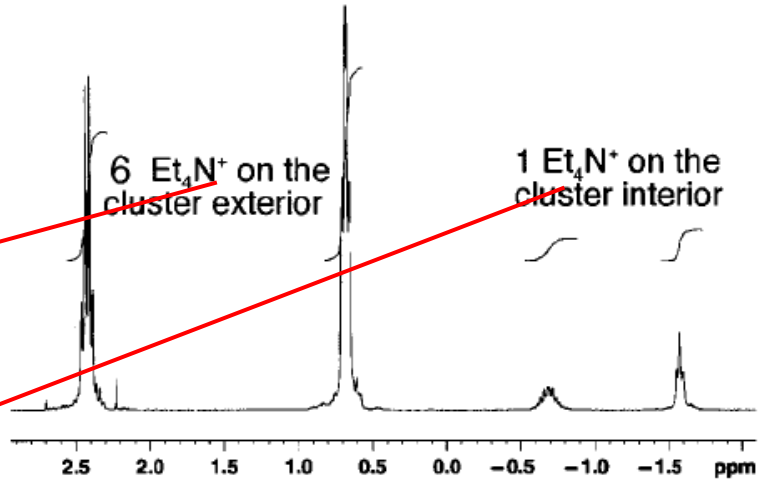


$^1$H NMR of $K_5(Et_4N)_7[Ga_4\mathbf{L}_6]$ depicting the two sets of $Et_4N^+$ resonances characteristic of the exterior and encapsulated cations.

K. N. Raymond et al., *J. Am. Chem. Soc.* **2001**, *123*, 8923.

# Heteroleptic Assemblies

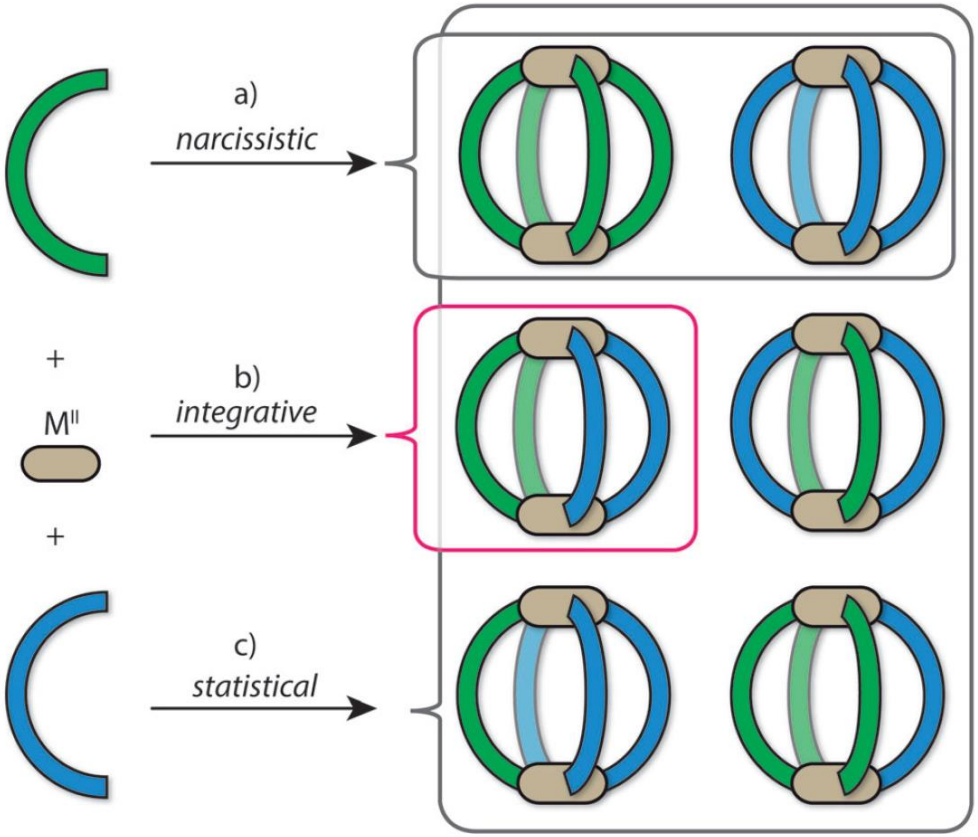


G. H. Clever et al., *Chem. Commun.* **2017**, *53*, 8506.

# Molecular Rectangles

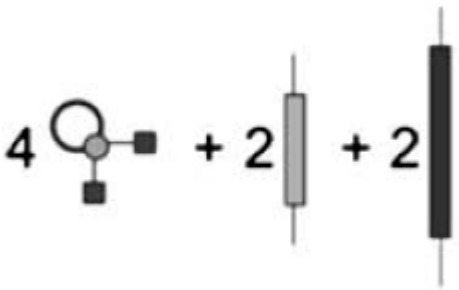


= blocking/directing ligand

= transition metal corner

= open coordination site

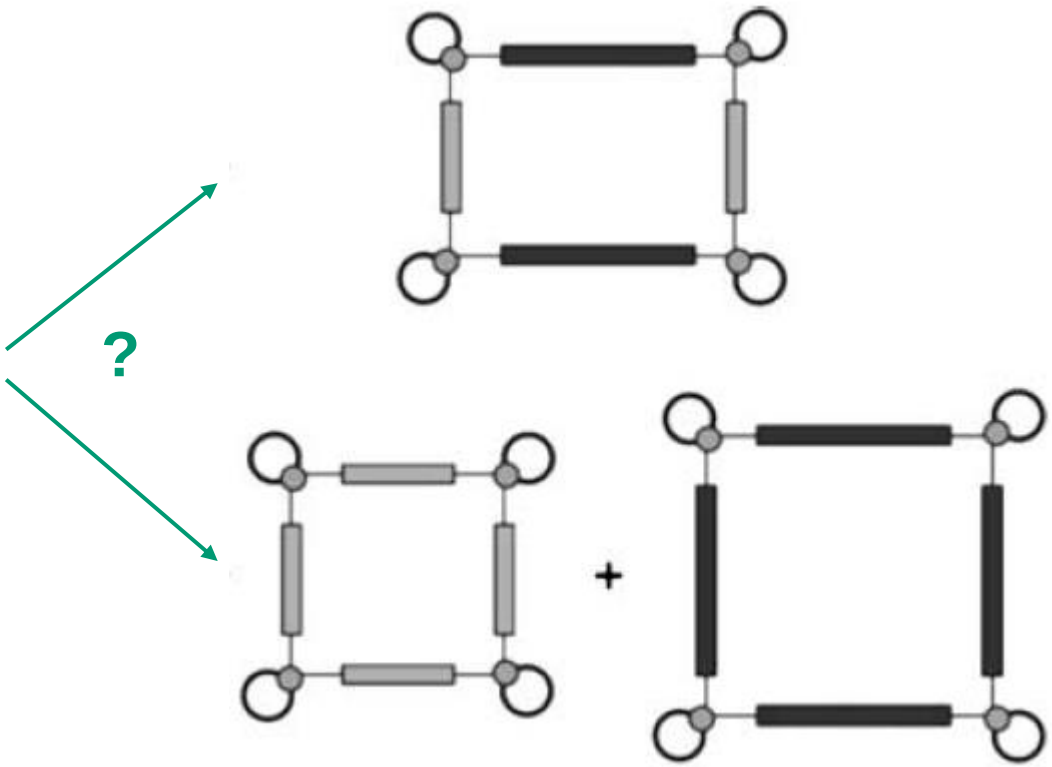

# Heteroleptic Assemblies

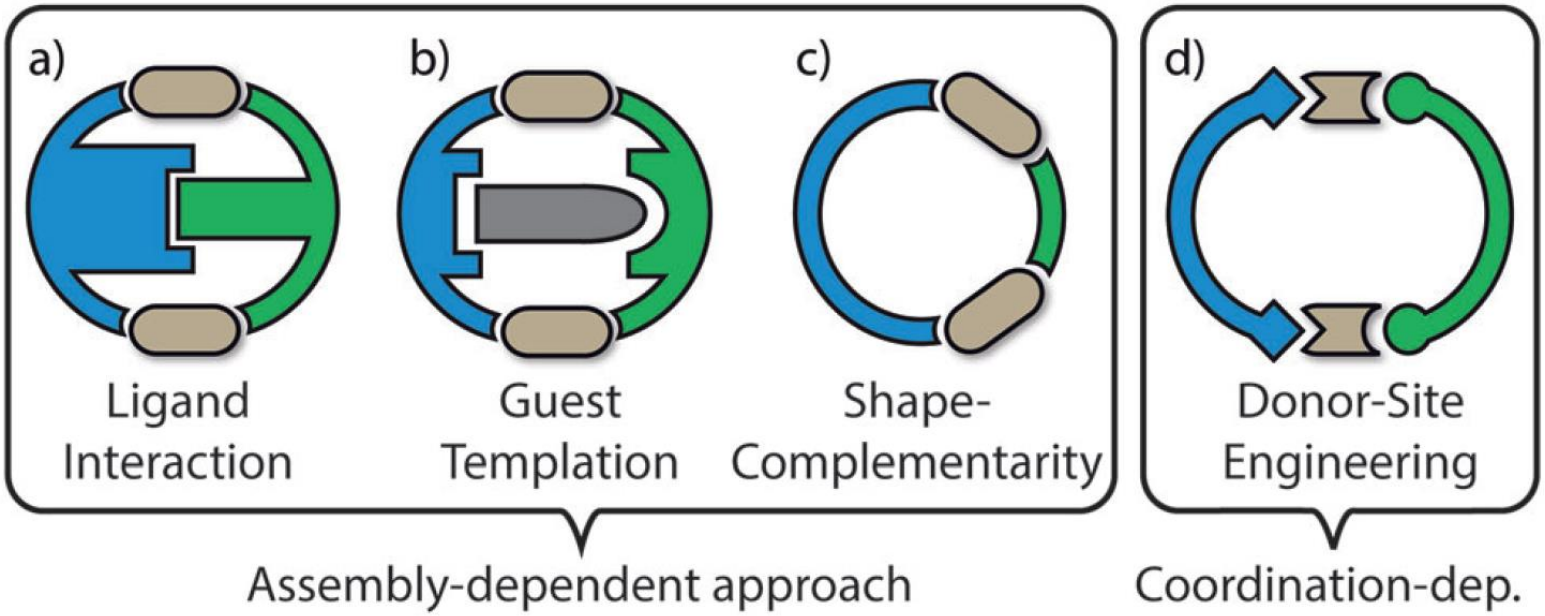


G. H. Clever et al., *Chem. Commun.* **2017**, *53*, 8506.

# Example: Shape-Complementarity

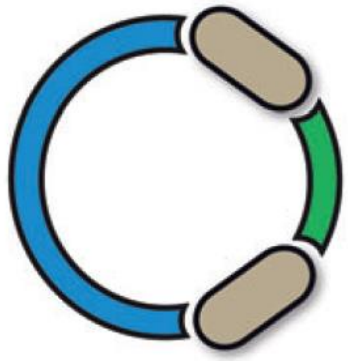

Shape-
Complementarity

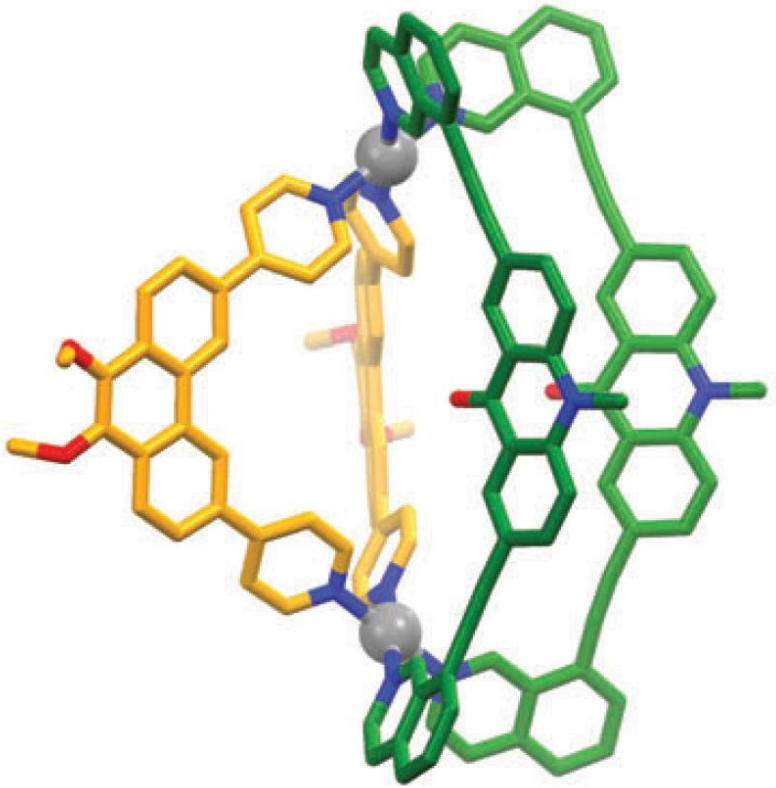

G. H. Clever et al., *J. Am. Chem. Soc.* **2016**, *138*, 13750.

# Low-Symmetry Ligands

= $Pd^{2+}$

= bridging ligand **L** with distinct binding sites

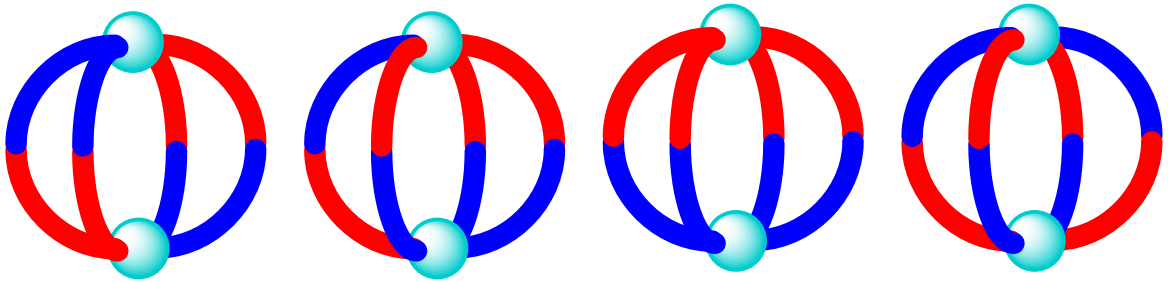

**4 Isomers**

# Low-Symmetry Ligands

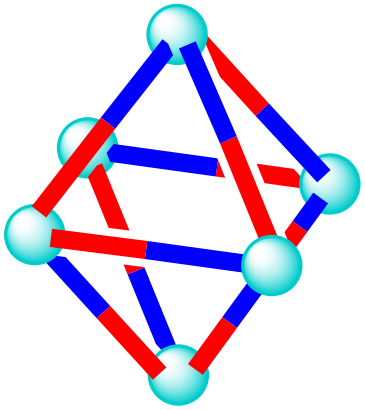

112 Isomers

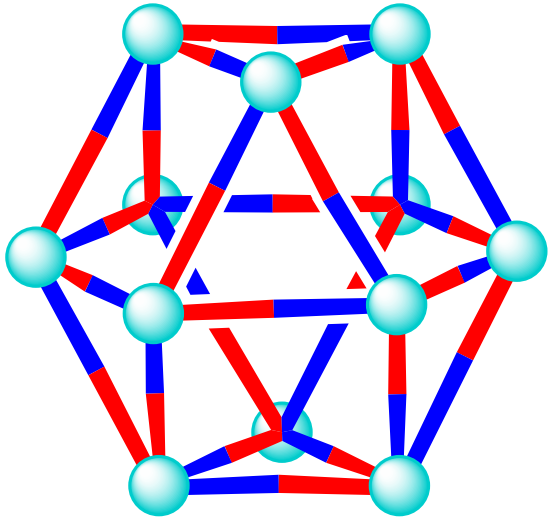

350'696 Isomers

# Orientational Self-Sorting in Cuboctahedral Assemblies

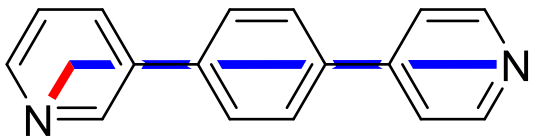


(2 eq.)

+

$[Pd(CH_3CN)_4](BF_4)_2$

(1 eq.)

$CD_3CN$

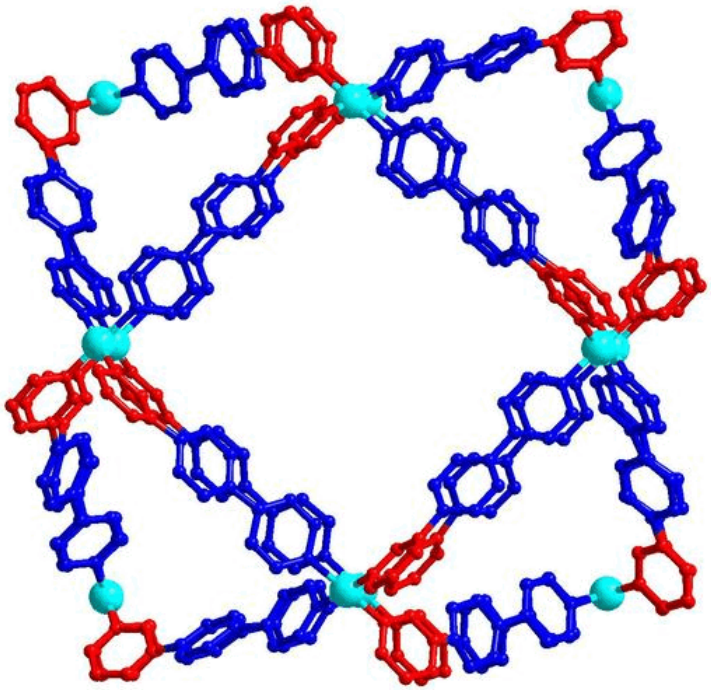

$C_{4h}$

K. Severin et al., *Chem. Sci.* **2022**, *13*, 11912.

# Helicates

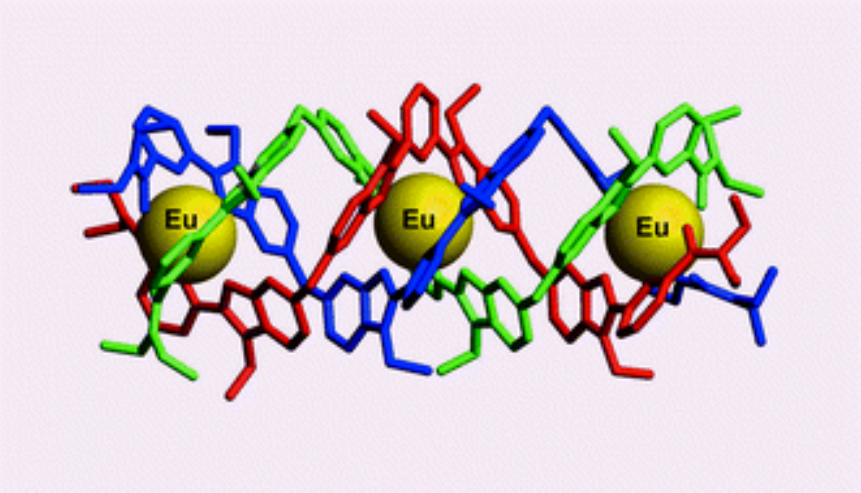


**Helicates**: “Discrete helical supramolecular complex constituted by one or more covalent organic strands wrapped about and coordinated to a series of ions defining the helical axis.”

“Strict self-assembly of polymetallic helicates: the concepts behind the semantics”
C. Piguet et al., *Coord. Chem. Rev.* **2005**, *249*, 705.

“Lets twist again — Double-stranded, triple-stranded and circular Helicates”
M. Albrecht, *Chem. Rev.* **2001**, *101*, 3457.

# Double-Stranded Helicates

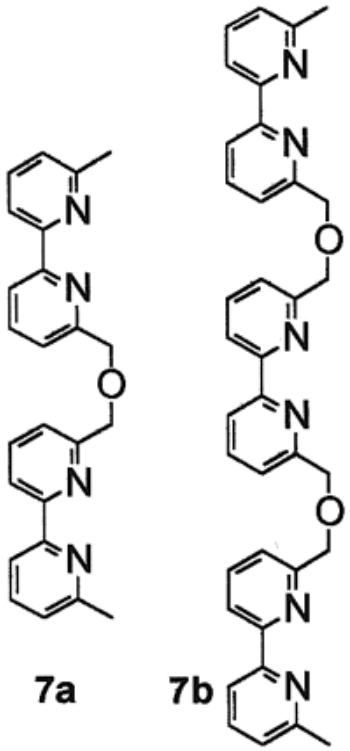



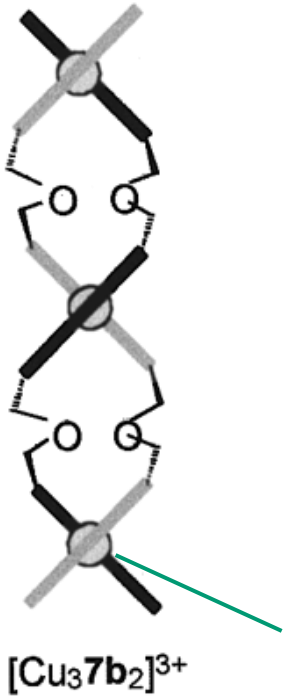


In 1987 Jean-Marie Lehn introduced the term double-stranded helicate for inorganic double helices in which two linear organic ligand strands are wrapping around two or more metal centers (some examples of helical double- or triple-stranded dinuclear complexes were already known). The bis(bipyridine) ligand **7a** and tris(bipyridine) ligand **7b** (Figure 4) were used to form dinuclear $[Cu_2\mathbf{7a}_2]^{2+}$ or trinuclear $[Cu_3\mathbf{7b}_2]^{3+}$ complexes with copper(I) ions.

Advantage of Cu(I): prefers tetrahedral coordination and NMR spectroscopy is possible (diamagnetic).

J.-M. Lehn et al., *Proc. Natl. Acad. Sci. U.S.A.* **1987**, *84*, 2565.

# A Triple-Stranded Helicate

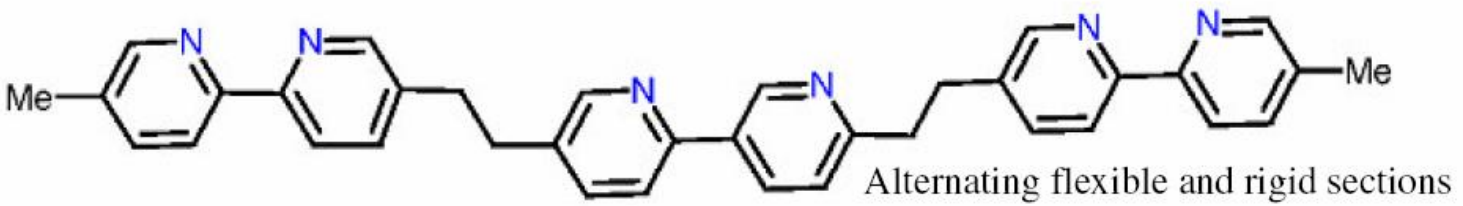


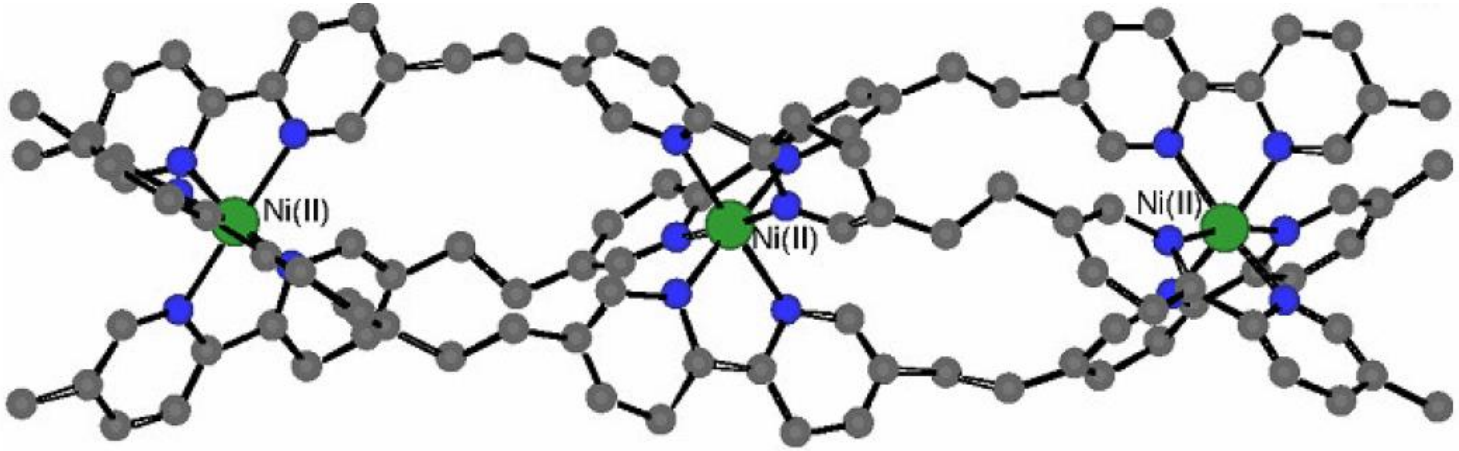


$Ni^{2+}$ gives labile complexes and thus facilitates error-correction processes.

J.-M. Lehn et al., *Angew. Chem. Int. Ed. Engl.* **1993**, *32*, 703.

# Circular Helicates

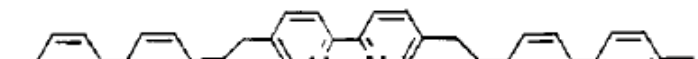

138

$FeCl_2$ Ethylene glycol 170°C

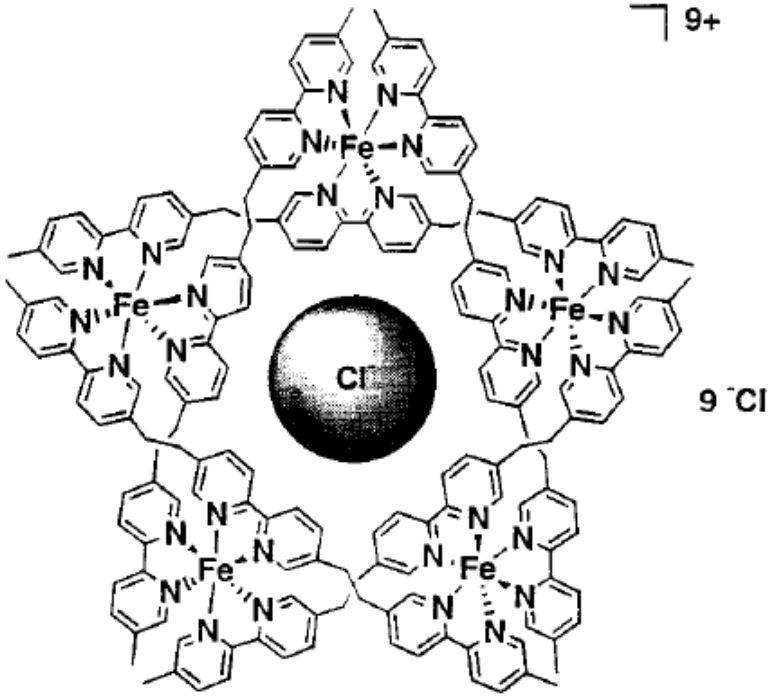


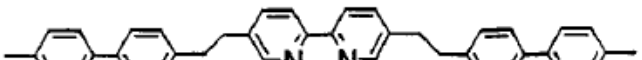

138

$FeSO_4$ $NH_4PF_6$ Ethylene glycol 170°C

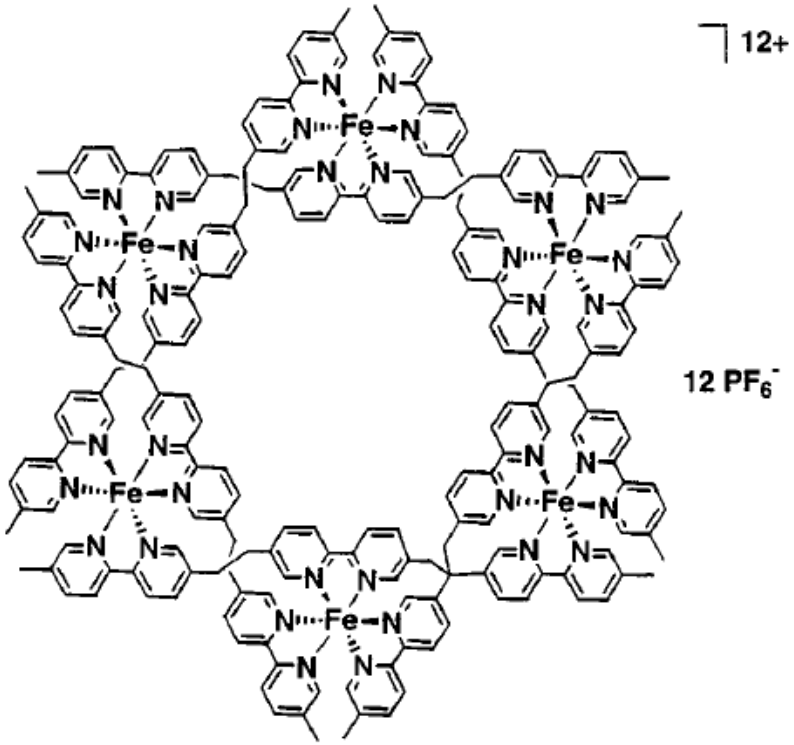

# Catecholate-Based Helicates

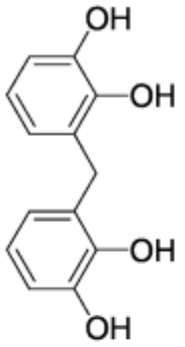


**9**

$Ti^{4+}$, base

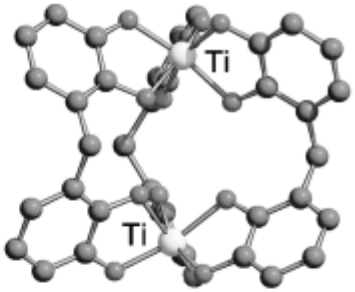


$[Ti_2\mathbf{9}_3]^{2-}$
(*meso*-helicate)

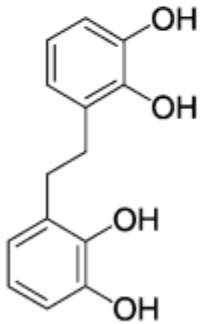


**10**

$Ti^{4+}$, base

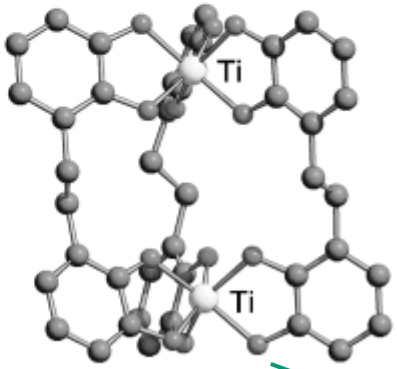


$[Ti_2\mathbf{10}_3]^{2-}$
(helicate)

Due to the zigzag-conformation of the alkyl-spacer, ligands with an odd number of methylene-units in the bridge lead to the achiral (!) *meso*-helicate; while ligands with an even number of $CH_2$ units are well predisposed for the formation of the helicate.

**$Ti^{4+}$ prefers hard O-donor ligands**

# Self-Recognition in Helicates

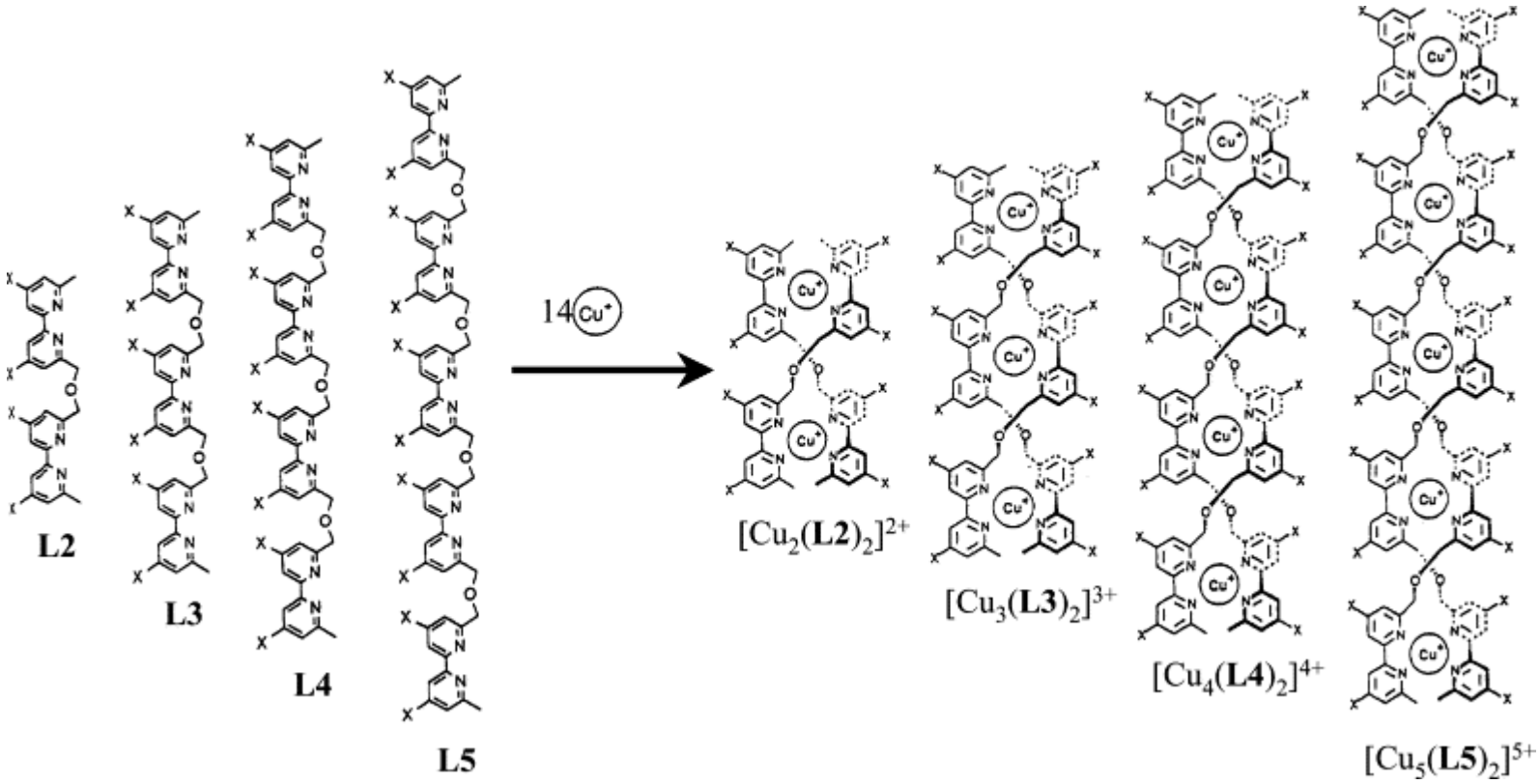


Self-recognition of the homopolymetallic double-stranded helicates. The self-sorting can be explained by considering enthalpic and entropic factors: a) the largest translational entropy results from the formation of a maximum number of short saturated oligomers; b) the maximum number of coordinative bonds minimizes the free energy.

# Molecular Grids

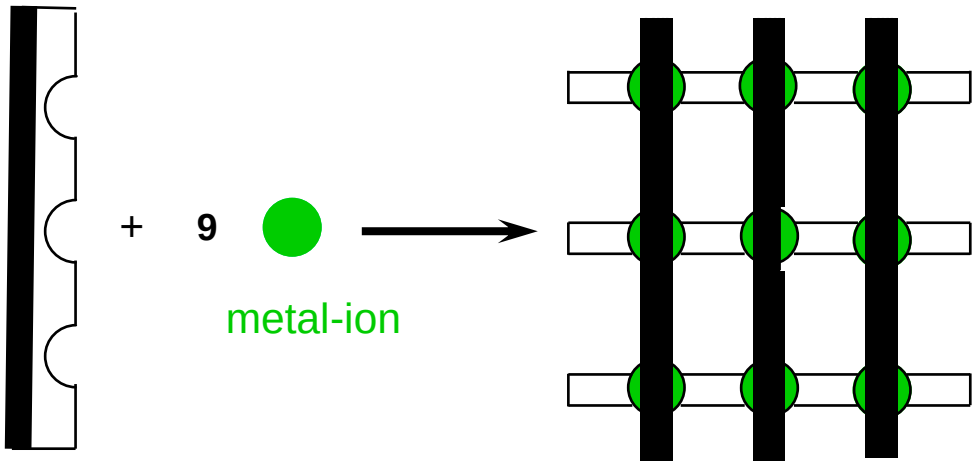


Periodic patterns

„Grid“

Transition-metal complexes of grid-type architecture comprise two-dimensional arrays of metal ions connected by a set of organic ligands in a perpendicular arrangement

“Grid-Type Metal Ion Architectures: Functional Metallosupramolecular Arrays”
J.-M. Lehn et al., *Angew. Chem. Int. Ed.* **2004**, *43*, 3644.

# Molecular Grids Based on Tetrahedral Coordination Geometries

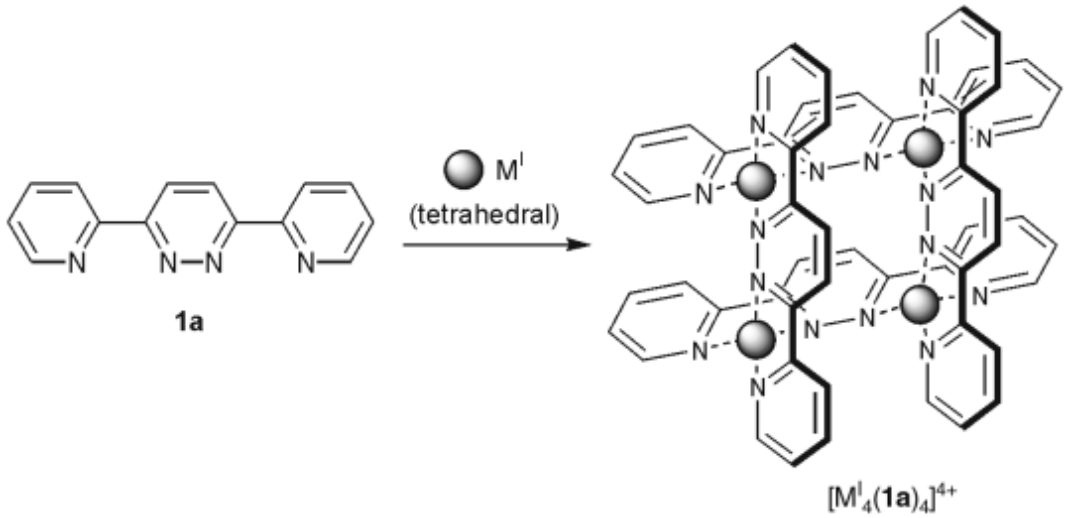


Schematic representation of the self-assembly process of ligand **1a** and tetrahedrally coordinating metal ions (M=Ag$^{I}$, Cu$^{I}$) leading to a [2×2] grid-type metalloarray $[M_4(\mathbf{1a})_4]^{4+}$. Both Cu$^{I}$ and Ag$^{I}$ ion arrays assemble spontaneously when the metal and ligand components are mixed in a 1:1 stoichiometry.

# Molecular Grids Based on Tetrahedral Coordination Geometries

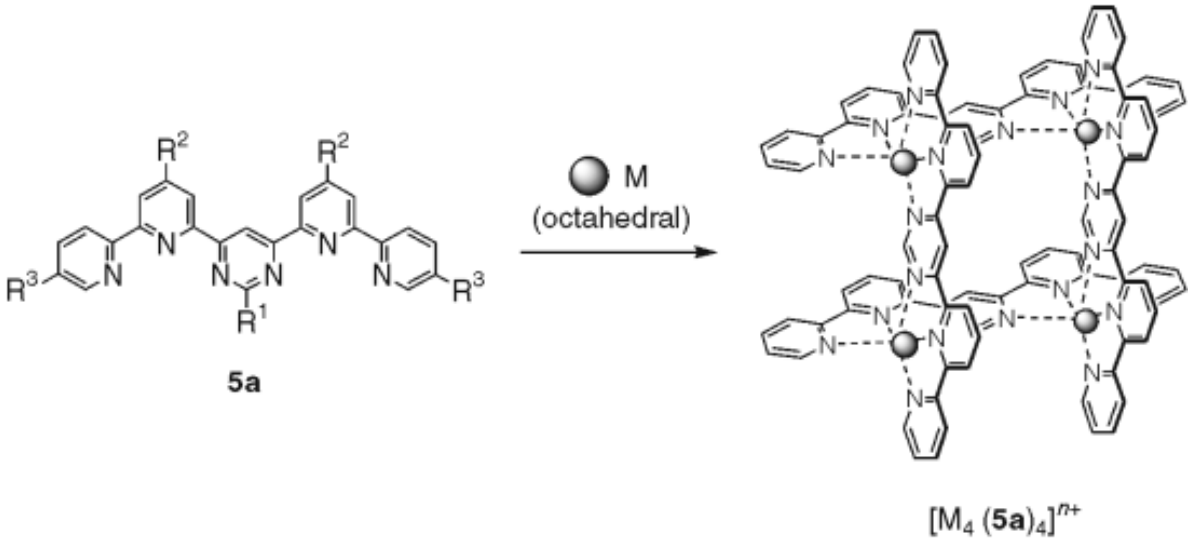


Ligand systems containing terpyridine-like coordination sites enable the arrangement of octahedrally coordinating metal ions: a number of late first- and second-row transition metal ions (e.g. $Mn^{II}$, $Co^{II}$, $Fe^{II}$, $Ni^{II}$, $Cu^{II}$, $Zn^{II}$, $Cd^{II}$) as well as some main group metal ions (e.g. $Pb^{II}$) have been introduced into gridlike arrays.

# A [4x4] Metal Ion Array

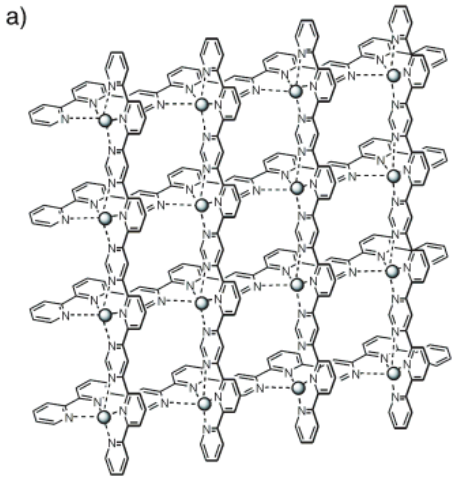


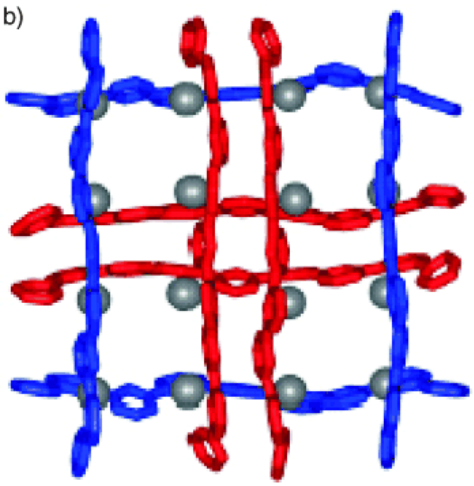


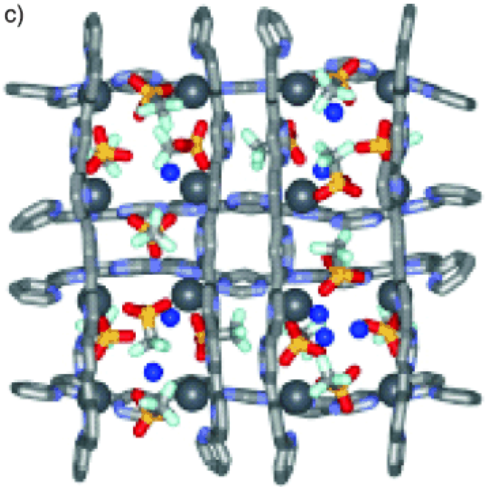


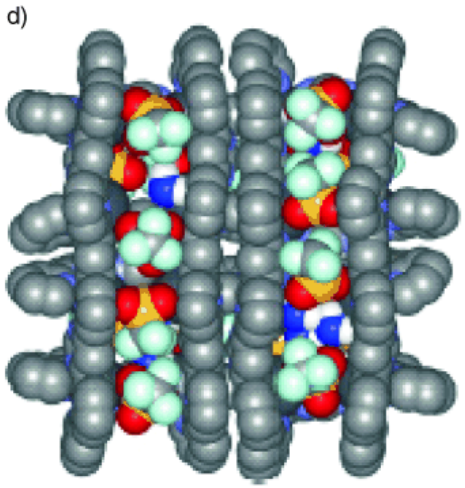


The largest square grid reported to date, $[Pb_{16}(\mathbf{L})_8](OTf)_{32}$, is formed quantitatively from eight equivalents of the tetratopic tridentate ligand **L** and sixteen equivalents of $Pb^{II}$ ions. This remarkable species arises from the self-organization of 24 precursors and involves the formation of 96 coordination bonds.

# Metallacrown Complexes

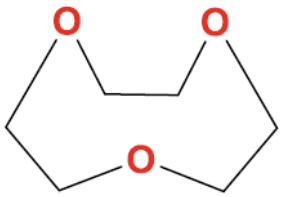


9-C-3

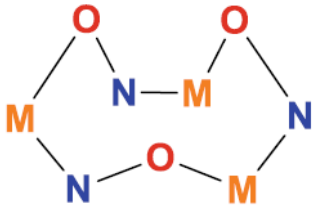


9-MC-3

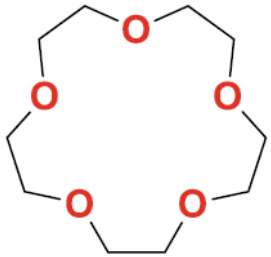


15-C-5

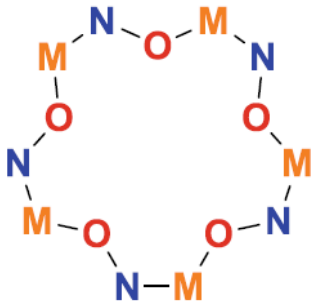


15-MC-5

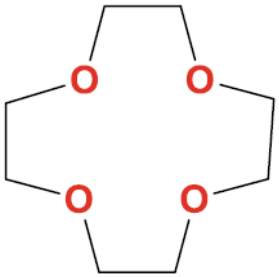


12-C-4

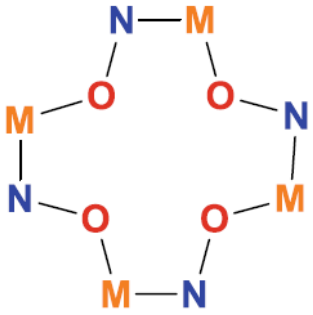


12-MC-4

Metallacrown complexes are analogues of crown ethers in which metal ions constitute an integral part of the macrocyclic framework.

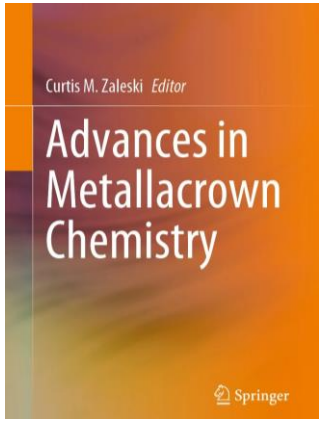


→ link

# Analogues of 12-Crown-3

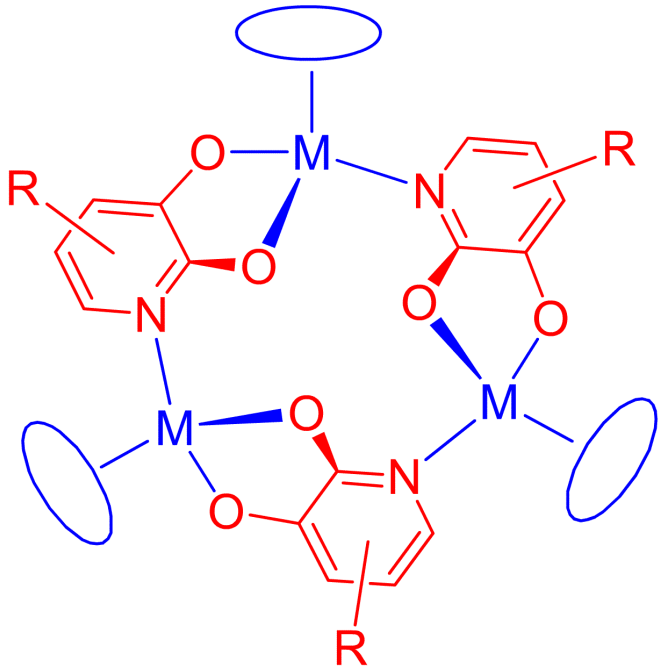


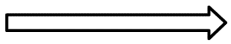

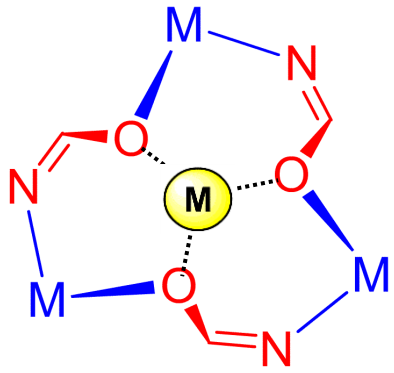


**12-Metallacrown-3**

**M = $Li^+$, $Na^+$**

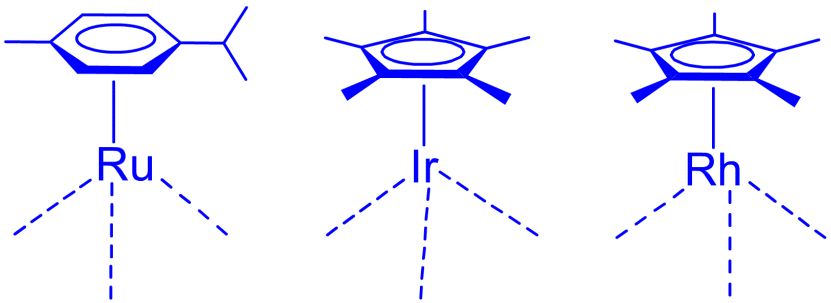


K. Severin,
*Coord. Chem. Rev.* **2003**, *245*, 3.

# Redox-Responsive Hosts

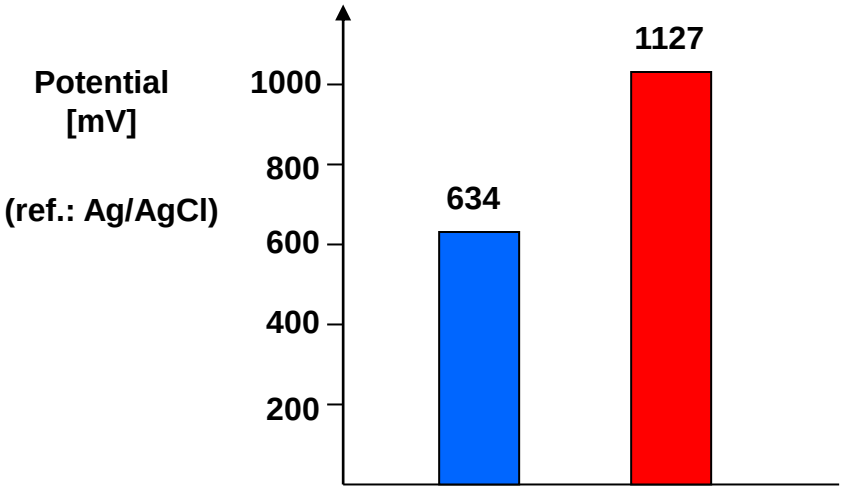


In the presence of $Li^+$, the metallacrown complex is more difficult to oxidize → potential application as an amperometric sensor.

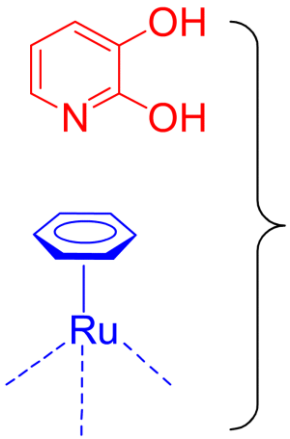


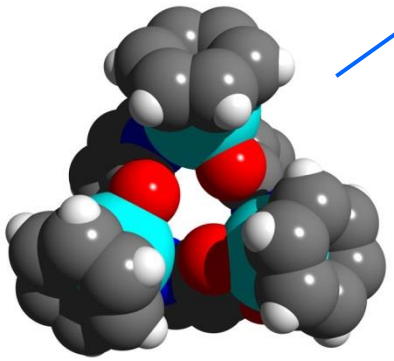

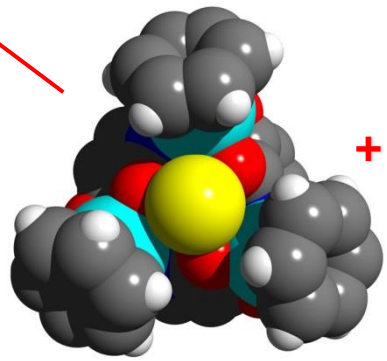

+ $Li^+$

# From Cages to Metal-Organic Frameworks

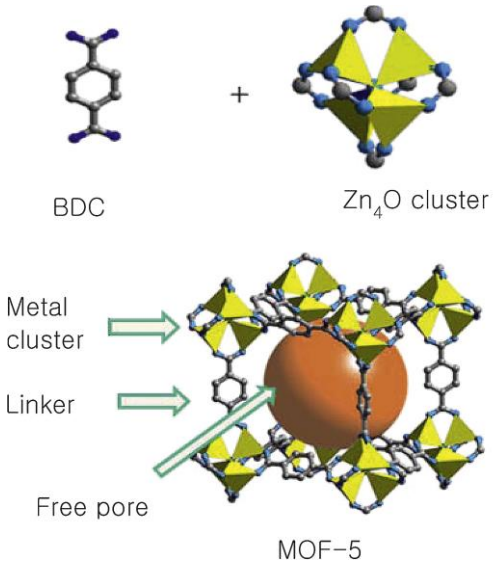


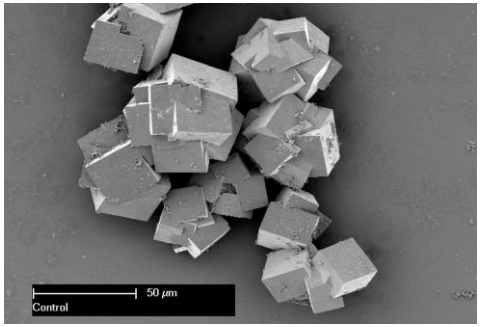


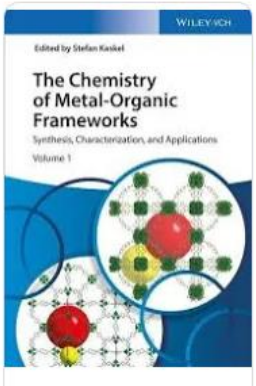


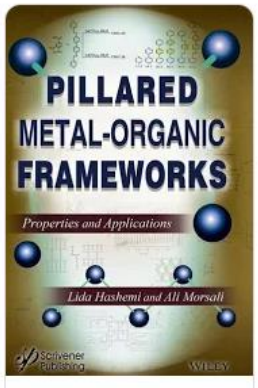


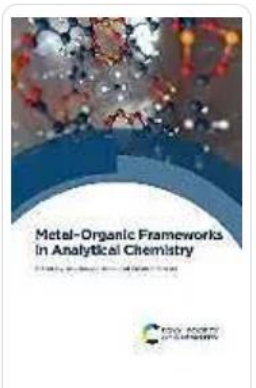


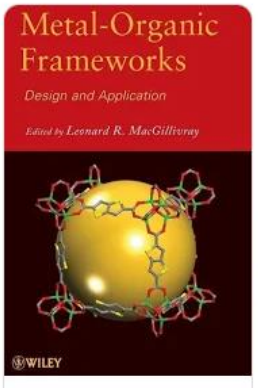



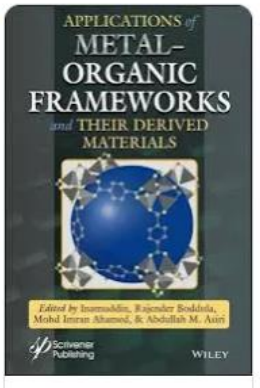


See the course of Prof. Wendy Queen (CH-450) → link